Estimations of Beam-Beam Fusion Reaction Rates in the Deuterium Plasma Experiment on LHD*)

Masayuki HOMMA, Sadayoshi MURAKAMI, Hideo NUGA and Hiroyuki YAMAGUCHI

Department of Nuclear Engineering, Kyoto University, Kyoto 615-8540, Japan

(Received 30 November 2015 / Accepted 6 June 2016)

Beam-beam nuclear fusion reactions in the Large Helical Device (LHD) deuterium plasma are investigated by the Global NEoclassical Transport (GNET) code, which can solve the five-dimensional drift kinetic equation using Monte Carlo methods. We evaluate the velocity space distribution of the energetic deuterons to calculate the fusion reaction rates between the beams. The calculated fraction of the beam-beam contribution is approximately 1.3% in the 1 MW heating power case and 6.7% in the 5 MW case, which would not be negligible. The beam-beam fusion rate depends on the square of the beam density and on the direction of the injected beams. When both the co- and counter-tangential beams are injected simultaneously, the synergetic beam-beam reaction rates can be approximately 2.9 times larger than the co-beamline contribution alone because of an increase in the relative velocity.

Keywords: LHD, deuterium experiment, NBI heating, beam-beam fusion reaction, GNET

DOI: 10.1585/pfr.11.2403109

1. Introduction

Experiments using deuterium plasmas are planned to examine the isotope effect on energy confinement or turbulent transport and to understand energetic ion confinement in the Large Helical Device (LHD). Plasma confinement is expected to be improved by use of deuterium plasmas. Therefore, it is important to understand the isotope effect for designing future fusion reactors.

During the D-D discharges, 1 MeV tritons and 2.5 MeV neutrons are generated via D-D fusion reactions, following which the confined tritons produce 14 MeV neutrons via triton burn-up. The confinement and slowing down of energetic tritons can be experimentally investigated by measuring the production rate of 14 MeV neutrons [1].

We have previously simulated the confinement of energetic tritons and triton burn-up in the D-D experiment on the LHD using the Global NEoclassical Transport (GNET) code [2, 3]. The D(d,p)T fusion reaction rates in the LHD deuterium plasma have been calculated by the FIT3D-DD code [4], which is an extended version of FIT3D. In the FIT3D-DD code, we have evaluated the fraction of tritons that are only produced via reactions between the deuterium beams from Neutral Beam Injection (NBI) heating and deuterium thermal ions, which are called beam-thermal reactions. Moreover, the effect of finite orbit width is not considered in FIT3D-DD.

In the deuterium plasma experiment, however, beam-beam reactions also occur, wherein both reacting ions are injected NBI deuterons. Therefore, it is necessary to estimate the contribution of the beam-beam fusion reactions with drift orbit effects to obtain more precise predictions of the triton burn-up ratios and the neutron production rates.

In this study, we estimate the beam-beam fusion reaction rates between the NBI deuteron beams in the deuterium plasma experiment on the LHD. We obtain the deuterium beam distribution functions using the GNET code, which solves the drift kinetic equation of energetic particles in a five-dimensional phase space, and the beam-beam fusion reaction rates are calculated. The radial profiles of the triton and neutron production rates are evaluated and compared with those of the beam-thermal contribution. In addition, we investigate their dependences on the plasma parameters.

2. Simulation Model

We apply the GNET code, which includes finite drift orbits and complicated motions of trapped particles, to solve the drift kinetic equation using Monte Carlo methods. The drift kinetic equation for beam deuterons in a five-dimensional phase space is described as follows:

$$\frac{\partial f_\mathrm{b}}{\partial t} + (\boldsymbol{v}_\parallel + \boldsymbol{v}_\mathrm{dr}) \cdot \frac{\partial f_\mathrm{b}}{\partial \boldsymbol{x}} + \dot{\boldsymbol{v}} \cdot \frac{\partial f_\mathrm{b}}{\partial \boldsymbol{v}} = C^\mathrm{coll}(f_\mathrm{b}) + L^\mathrm{particle}(f_\mathrm{b}) + S_\mathrm{b}, \quad (1)$$

where f_b is the distribution function of the beam deuterons, $\boldsymbol{v}_\parallel$ is the velocity parallel to the field line, $\boldsymbol{v}_\mathrm{dr}$ is the drift velocity, $C^\mathrm{coll}(f_\mathrm{b})$ is a linear Coulomb collision operator, L^particle is the particle loss term from the last closed flux surface (LCFS), and S_b is the source term for the NBI deuterons. We calculate the birth profile of the NBI

author's e-mail: homma@p-grp.nucleng.kyoto-u.ac.jp

*) This article is based on the presentation at the 25th International Toki Conference (ITC25).

deuteron beams using the HFREYA code [5].

We calculate the D(d,p)T fusion reaction rates using the distribution functions of the NBI deuterons obtained from GNET. The averaged reaction rates of the D(d,p)T reaction can be separated into different components. The beam-thermal term $Y_{\text{b-th}}$ and the beam-beam term $Y_{\text{b-b}}$ can be expressed as

$$Y_{\text{b-th}} = n_{\text{b}} n_{\text{th}} \langle \sigma v \rangle_{\text{b-th}}, \tag{2}$$

$$Y_{\text{b-b}} = \begin{cases} n_{\text{b}_i} n_{\text{b}_j} \langle \sigma v \rangle_{\text{b-b}} & (i \neq j) \\ \frac{1}{2} n_{\text{b}_i}^2 \langle \sigma v \rangle_{\text{b-b}} & (i = j) \end{cases}, \tag{3}$$

where

$$\langle \sigma v \rangle_{12} = \iint f_1(\boldsymbol{v}_1) f_2(\boldsymbol{v}_2) \sigma(E) |\boldsymbol{v}_1 - \boldsymbol{v}_2| \mathrm{d}\boldsymbol{v}_1 \mathrm{d}\boldsymbol{v}_2. \tag{4}$$

Here, n_{b_i} (n_{b_j}) and n_{th} denote the density of the beam deuterons from the i-th (j-th) beamline and the thermal ion density, respectively. The suffixes 1 and 2 in Eq. (4) represent either the thermal or the beam deuterons. The cross section σ is given as follows [6]:

$$\sigma(E) = \frac{\left[\left(1.220 - 4.36 \times 10^{-4} E\right)^2 + 1\right]^{-1} \times 372}{E\left[\exp\left(46.097 E^{-\frac{1}{2}}\right) - 1\right]}, \tag{5}$$

where E is the deuteron kinetic energy for the relative velocity.

3. Simulation Results

The beam-thermal and beam-beam D(d,p)T fusion rates in the deuterium plasma experiment on the LHD are calculated assuming typical values for the plasma parameters: core electron temperature $T_{\text{e}}(0) = 3.0\,\text{keV}$; edge electron temperature $T_{\text{e}}(a) = 0.1\,\text{keV}$; core ion temperature $T_{\text{i}}(0) = 3.0\,\text{keV}$; edge ion temperature $T_{\text{i}}(a) = 0.1\,\text{keV}$; core electron density $n_{\text{e}}(0) = 0.8, 2.0$, and $3.5 \times 10^{19}\,\text{m}^{-3}$; edge electron density $n_{\text{e}}(a) = 0.1 \times 10^{19}\,\text{m}^{-3}$; magnetic field strength $B_0 = 2.75\,\text{T}$; magnetic axis major radius $R_{\text{ax}} = 3.50, 3.60$, and $3.75\,\text{m}$; and beta value $\beta = 0.23\%$. The LHD experiments are performed for various magnetic configurations because the confinement of trapped particles is strongly improved by an inward shift of the magnetic axis [7]. The radial profiles of the plasma temperature and density are given by

$$T_{\text{e}}(r) = (T_{\text{e}}(0) - T_{\text{e}}(a))\left[1 - \left(\frac{r}{a}\right)^2\right] + T_{\text{e}}(a), \tag{6}$$

$$n_{\text{e}}(r) = (n_{\text{e}}(0) - n_{\text{e}}(a))\left[1 - \left(\frac{r}{a}\right)^8\right] + n_{\text{e}}(a). \tag{7}$$

The bulk plasma is assumed to be a deuterium-hydrogen mixed plasma with the density ratio of $n_{\text{D}}/(n_{\text{D}} + n_{\text{H}}) = 0.8$. We assume a balance between the beam particle source, the thermalization, and the outward flux.

Five NBI heating systems are installed in the LHD: three tangential injection beams ($E_{\text{b}} = 180\,\text{keV}$) and two perpendicular beams ($E_{\text{b}} = 60 - 80\,\text{keV}$). The injected energy is much higher for the tangential injection beams, and the fusion reactions due to the tangential beams are dominant in the LHD deuterium plasma experiments. Assuming the co-tangential injection beam and the counter-tangential beam with energy $E_{\text{b}} = 180\,\text{keV}$, we evaluate the quantities per megawatt of heating power. We consider beam ions whose energies are greater than $3T_{\text{i}}(r)$ to be reactants when calculating the beam-beam fusion rates.

3.1 Beam deuteron distribution

Applying the source term calculated by the HFREYA code for GNET, we evaluate the beam deuteron distribution in velocity and real spaces. First, we calculate a typical case for the density of $n_{\text{e}}(0) = 2.0 \times 10^{19}\,\text{m}^{-3}$ and the magnetic configuration with $R_{\text{ax}} = 3.60\,\text{m}$. The velocity distribution of the beam deuterons from the co-NB is presented

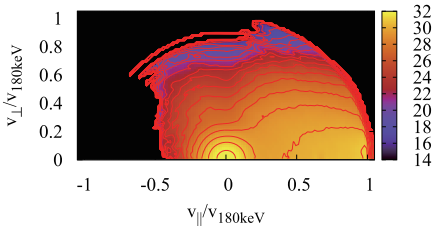

Fig. 1 Contours of the velocity distribution function of the beam deuterons for the co-NB.

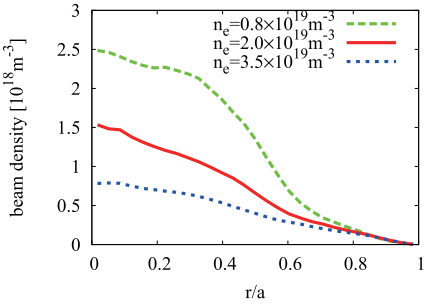

(a) Plasma density dependence

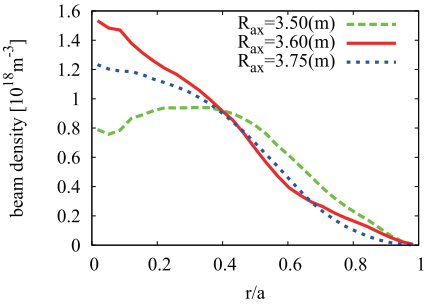

(b) Magnetic configuration dependence

Fig. 2 Radial profile of the beam deuteron density with different (a) plasma densities ($n_{\text{e}}(0) = 0.8, 2.0$, and $3.5 \times 10^{19}\,\text{m}^{-3}$) and (b) magnetic configurations ($R_{\text{ax}} = 3.50, 3.60$, and $3.75\,\text{m}$).

in Fig. 1. Here $v_{\parallel}$ and $v_{\perp}$ represent the parallel and perpendicular velocity components relative to the magnetic field direction, respectively, which are normalized by the velocity of 180 keV deuterons $v_{180\,\mathrm{keV}}$.

In Fig. 2, the radial profiles of the NBI deuteron density are shown for various values of plasma density and magnetic configuration. Here we assume the co-NBI heating system with the power of 1 MW. The magnetic axis position for Fig. 2 (a) is $R_{\mathrm{ax}} = 3.60$ m and the plasma density for Fig. 2 (b) is $n_{\mathrm{e}}(0) = 2.0 \times 10^{19}\,\mathrm{m}^{-3}$. The slowing-down time for the beam ions due to collisions with the background plasma depends inversely on the plasma density. Hence, the slowing-down time is longer in the lower density case and the beam deuteron density becomes larger. In the $R_{\mathrm{ax}} = 3.50$ m case, the confinement of the trapped particles is improved; however, the core beam density is lower because the NBI system is designed so that the center of the beamline passes through the position of the major radius $R = 3.60 - 3.75$ m. A comparison between the NBI deuteron density profiles of the co-tangential and counter-tangential beamlines is presented in Fig. 3, and typical orbits of the passing beam deuterons in the poloidal cross section are shown in Fig. 4. We assume typical plasma parameters of the density $n_{\mathrm{e}}(0) = 2.0{\times}10^{19}\,\mathrm{m}^{-3}$ and magnetic configuration $R_{\mathrm{ax}} = 3.60$ m in both figures. In Fig. 4, the direction of the magnetic field is downward orthogonal to the page, and the direction of the ∇B is leftward parallel to the page. The poloidal drift motion is in opposite directions for the co- and counter-passing particles. As a consequence, the orbits of the deuterons from the counter-NB tend to deviate from the central region.

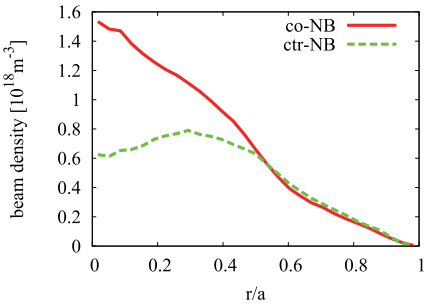

Fig. 3 Dependence of the beam deuteron density profile on the NBI beamlines.

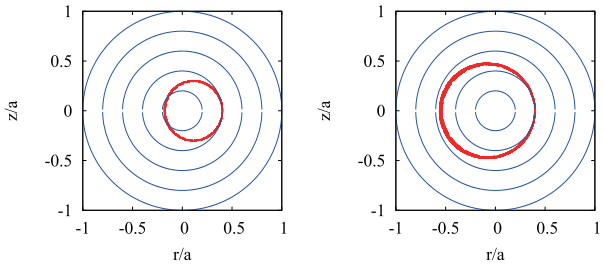

(a) Passing particle with $v_{\parallel} > 0$ (b) Passing particle with $v_{\parallel} < 0$

Fig. 4 Typical orbits of a passing beam particle with (a) $v_{\parallel} > 0$ ($\theta_{\mathrm{p}} = 10°$) and (b) $v_{\parallel} < 0$ ($\theta_{\mathrm{p}} = 170°$).

3.2 Beam-thermal reaction rates

We evaluate the D-D fusion reaction rates by applying the velocity distribution of the deuteron beams obtained from the GNET code. In Fig. 5, the radial profiles of the evaluated neutron production rates due to the beam-thermal fusion reactions are presented in different plasma densities and magnetic configurations. Here again, the co-NB system is assumed with the heating power of 1 MW. It is found that the neutron production rate does not simply depend on the plasma density because the population of energetic beam ions depends on the beam ion birth and slowing-down processes. The highest production rate occurs at $n_{\mathrm{e}}(0) = 2.0 \times 10^{19}\,\mathrm{m}^{-3}$, which would result from the combination of the beam birth profile and the background density. Integrated over the plasma volume, the total neutron emissivity due to beam-thermal reactions is approximately $6.6 \times 10^{14}\,\mathrm{s}^{-1}$ per megawatt for the typical plasma parameters. In Fig. 6, the beam-thermal fusion reaction rates are compared between the co- and counter-injected beamlines in the case with $n_{\mathrm{e}}(0) = 2.0 \times 10^{19}\,\mathrm{m}^{-3}$ and $R_{\mathrm{ax}} = 3.60$ m. The difference in the beam-thermal reaction rates is caused by changes in the beam orbits.

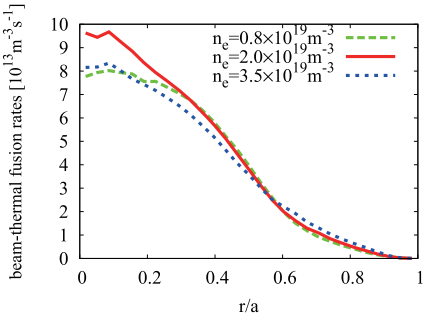

(a) Plasma density dependence

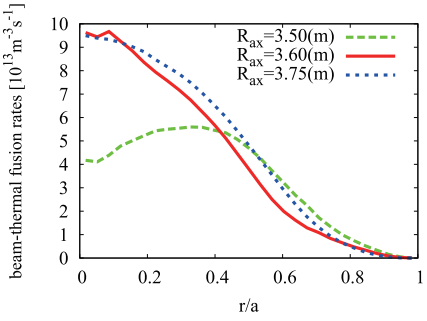

(b) Magnetic configuration dependence

Fig. 5 Radial profile of the beam-thermal reaction rates with different (a) plasma densities ($n_{\mathrm{e}}(0) = 0.8, 2.0$, and $3.5 \times 10^{19}\,\mathrm{m}^{-3}$) and (b) magnetic configurations ($R_{\mathrm{ax}} = 3.50, 3.60$, and 3.75 m).

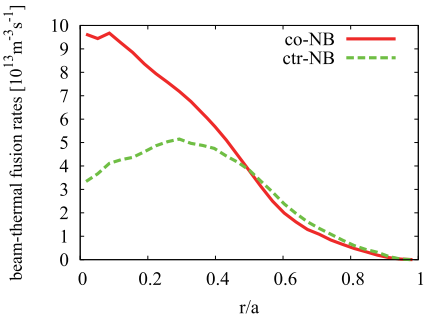

Fig. 6 Dependence of the beam-thermal reaction rates on the NBI beamlines.

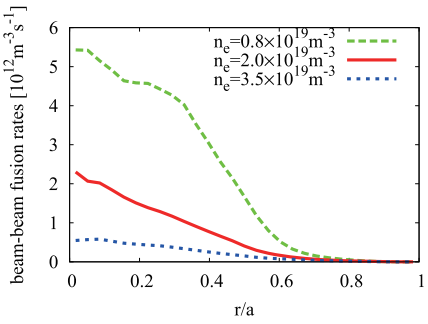

(a) Plasma density dependence

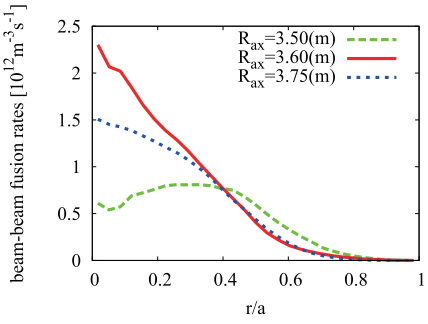

(b) Magnetic configuration dependence

Fig. 7 Radial profile of the beam-beam reaction rates with different (a) plasma densities ($n_e(0) = 0.8, 2.0$, and $3.5 \times 10^{19}\,\mathrm{m}^{-3}$) and (b) magnetic configurations ($R_{ax} = 3.50, 3.60$, and $3.75\,\mathrm{m}$).

3.3 Beam-beam reaction rates

Next we evaluate the beam-beam fusion reaction rates. In Fig. 7, the radial profiles of the evaluated neutron production rates due to the beam-beam fusion reactions are presented for various densities and magnetic configurations. Comparing them to Fig. 2, we can see that the beam-beam fusion rate is nearly proportional to the square of the beam density. For example, when $R_{ax} = 3.50\,\mathrm{m}$, the central beam density and the beam-beam reaction rate are approximately 0.51 times and 0.27 times greater, respectively, than the density and reaction rate when $R_{ax} = 3.60\,\mathrm{m}$.

The beam-beam fusion rates are then compared to the beam-thermal contribution. Figure 8 (a) shows a comparison between the beam-beam and beam-thermal contributions for a case with 1 MW heating power assuming the typical plasma parameters $n_e(0) = 2.0 \times 10^{19}\,\mathrm{m}^{-3}$ and $R_{ax} = 3.60\,\mathrm{m}$. The calculated ratio of the beam-beam contribution to the total D-D reaction rate is 1.3%. This ratio is 4.5% when $n_e(0) = 0.8 \times 10^{19}\,\mathrm{m}^{-3}$ and 0.45% when $n_e(0) = 3.5 \times 10^{19}\,\mathrm{m}^{-3}$. The result in the case with 5 MW NBI power is presented in Fig. 8 (b). When the beam power is added to 5 MW, the beam-beam reaction rate increases by approximately 25 times. Therefore, the beam-beam fusion rate is nearly proportional to the heating power squared.

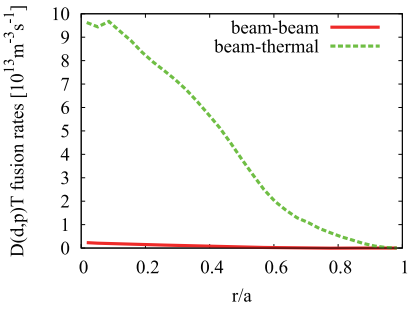

(a) NBI power of 1 MW

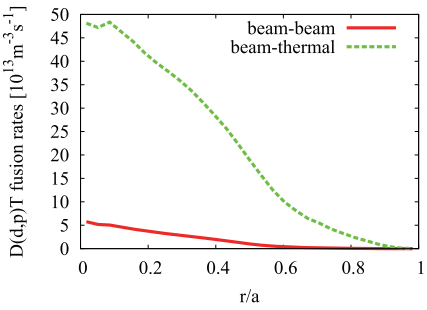

(b) NBI power of 5 MW

Fig. 8 Comparison between the beam-beam and beam-thermal contributions for heating powers of (a) 1 MW and (b) 5 MW.

Finally, we investigate the situation where the co- and counter-NBs coexist. Figure 9 shows the beam-beam reaction rates between deuterons from the co-NB and the counter-NB (total 2 MW) along with each beam contribution (2 MW each). The beam-beam fusion rate due to the co-NB alone, integrated over the plasma volume, is approximately $3.5 \times 10^{13}\,\mathrm{s}^{-1}$ and the rate due to the counter-NB is approximately $1.9 \times 10^{13}\,\mathrm{s}^{-1}$. Meanwhile, the synergetic beam-beam fusion rate between the co- and counter-NBs is approximately $1.0 \times 10^{14}\,\mathrm{s}^{-1}$. When both the co- and counter-NBs are injected simultaneously, the synergetic beam-beam fusion rate can be a factor of 2.9 larger than the co-NB contribution alone, which is reasonable due to the resulting increase in the relative velocity in Eq. (4).

The two co-NBs and one counter-NB are applied on the LHD and the heating power is 5 MW for each. In this case, the synergetic beam-beam fusion rate between the

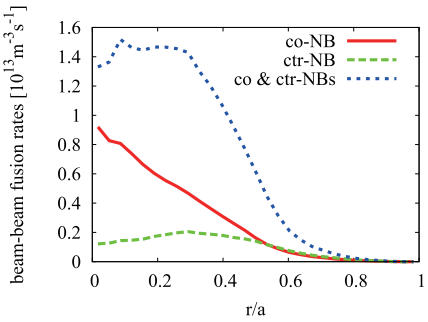

Fig. 9 Beam-beam reaction rates between the deuterons from the co- and counter-NBs (total 2 MW) along with each beam contribution (2 MW each).

two co-NBs and the one counter-NB is approximately 50 times the rate shown in Fig. 9 and is calculated to be 5.2×10^{15} s^{-1}. This can be equivalent to approximately 1.6 times the beam-thermal reaction rate for one co-NB with 5 MW heating power.

4. Conclusions

We have evaluated the beam-beam fusion reactions in the LHD plasma during the D-D experiment and compared them to the beam-thermal contribution. To calculate the fusion rates, we have applied the velocity distribution functions of the beam ions obtained using GNET, the five-dimensional drift kinetic equation solver.

We have found that the beam-thermal fusion rate does not have a simple dependence on the plasma density and that it becomes lower for the inward shifted configuration. In addition, the beam-beam fusion rate is dependent on the square of the beam density and the heating power. The ratio of the beam-beam contribution has been calculated to be approximately 1.3% when the heating power is 1 MW. Furthermore, the nonlinear fusion rate between the co- and counter-beam deuterons can be 2.9 times larger than the co-NB contribution alone. In the experimental condition of two co-NBs and one counter-NB with 5 MW power each, the production rate of the D-D neutrons due to the synergetic effects of the combined injection can be 1.6 times the beam-thermal reaction rate of one co-NB.

[1] T. Nishitani *et al.*, Plasma Phys. Control. Fusion **38**, 355 (1996).
[2] S. Murakami *et al.*, Nucl. Fusion **40**, 693 (2000).
[3] Y. Masaoka *et al.*, Nucl. Fusion **53**, 093030 (2013).
[4] M. Homma *et al.*, Plasma Fusion Res. **10**, 3403050 (2015).
[5] S. Murakami, Trans. Fusion Technol. **27**, 256 (1995).
[6] J. D. Huba, *NRL Plasma Formulary* (Naval Research Laboratory, 2002).
[7] S. Murakami *et al.*, Nucl. Fusion **42**, L19 (2002).